Sparsity-Based Estimation for Target Detection in Multipath Scenarios†

Satyabrata Sen, Gongguo Tang, and Arye Nehorai
Department of Electrical and Systems Engineering
Washington University in St. Louis
One Brookings Drive, St. Louis, MO 63130, USA
Email: {ssen3, gt2, nehorai}@ese.wustl.edu
Phone: 314-935-7520 Fax: 314-935-7500

***Abstract*—We propose a sparsity-based estimation approach for detecting a moving target in multipath scenarios. We employ an orthogonal frequency division multiplexing (OFDM) radar to increase the frequency diversity of the system. Moreover, the multipath propagation increases the spatial diversity by providing extra looks at the target. First, we exploit the sparsity of multiple paths and the knowledge of the environment to develop a parametric OFDM radar model at a particular range cell. Then, to estimate the sparse vector, we apply a collection of multiple small Dantzig selectors (DS). We use the ℓ_1-constrained minimal singular value (ℓ_1-CMSV) of the measurement matrix to analytically evaluate the reconstruction performance and demonstrate that our decomposed DS performs better than the standard DS. We provide a few numerical examples to illustrate the performance characteristics of the sparse recovery.**

***Index Terms*—Target detection, OFDM radar, sparse estimation, Dantzig selector, ℓ_1-constrained minimal singular value.**

I. Introduction

The problem of detecting a target in multipath scenarios, particularly in urban environments, is becoming increasingly relevant to radar technologies. In [1], [2], we showed that the target-detection capability can be significantly improved by exploiting multiple Doppler shifts corresponding to the projections of the target velocity on each of the multipath components. To resolve and exploit the multipath components, we consider an orthogonal frequency division multiplexing (OFDM) signalling scheme [3]. The use of an OFDM signal mitigates possible fading, resolves multipath reflections, and provides additional frequency diversity as different scattering centers of a target resonate at different frequencies.

In this work, we consider a target-detection problem in multipath scenarios from a different perspective (see also [4]). We observe that the radar receives the target information through a LOS, several reflected paths, or both. Therefore, using our knowledge of the geometry, we can determine all the possible paths, be they LOS or reflected, and the associated target locations corresponding to a particular range cell. Then, considering the presence of a single target, we can apply any sparse-signal recovery algorithm [5]-[7] to determine the paths along which the target response is received. Thus, we transform the target-detection problem into the task of estimating the spectrum of a sparse signal.

First, in Section II we develop a parametric OFDM measurement model for a particular range cell, to detect a far-field point target moving in a multipath-rich environment. For simplicity we consider only first-order specularly reflected multipath signals. Then, we convert the model to a sparse model that accounts for the target returns over all possible signal paths and target velocities. The nonzero components of the sparse vector correspond to the scattering coefficients of the target at different OFDM subcarriers. We assume that the clutter and measurement noise are temporally white.

To estimate the sparse vector, we propose a sparse-recovery algorithm based on the Dantzig selector (DS) approach [7] in Section III. The DS approach belongs to the class of convex relaxation methods in which the ℓ_0 norm is replaced by the ℓ_1 norm that remains a measure of sparsity while being a convex function. Other examples of convex relaxation methods include the basis pursuit [5] and LASSO estimator [8]. However, instead of using the standard DS, we employ a collection of multiple small DS to exploit more prior structures of the sparse vector. Furthermore, we analytically evaluate the performance characteristics and show that our decomposed DS has advantages over the standard DS both in terms of computation and performance. To analyze the reconstruction performance we consider the ℓ_1-constrained minimal singular value (ℓ_1-CMSV) of the measurement matrix [9]. Compared with the traditional restricted isometry constant (RIC) [10], [11], which is extremely difficult to compute for an arbitrarily given matrix, the ℓ_1-CMSV is an easily computable measure and provides more intuition on the stability of sparse-signal recovery. More importantly, in [9] we already designed several algorithms to compute the ℓ_1-CMSV of any given measurement matrix.

We present several numerical examples to illustrate the sparse-estimation performance for a target-detection problem in Section IV. We evaluate the performance characteristics in terms of normalized root mean squared error (RMSE) and empirical receiver operating characteristic (ROC). We show that the decomposed DS performs better than the standard

† This work was supported by the Department of Defense under the Air Force Office of Scientific Research MURI Grant FA9550-05-1-0443, ONR Grant N000140810849, and NSF Grant CCF-1014908.

978-1-4244-8902-2/11/$26.00 ©2011 IEEE

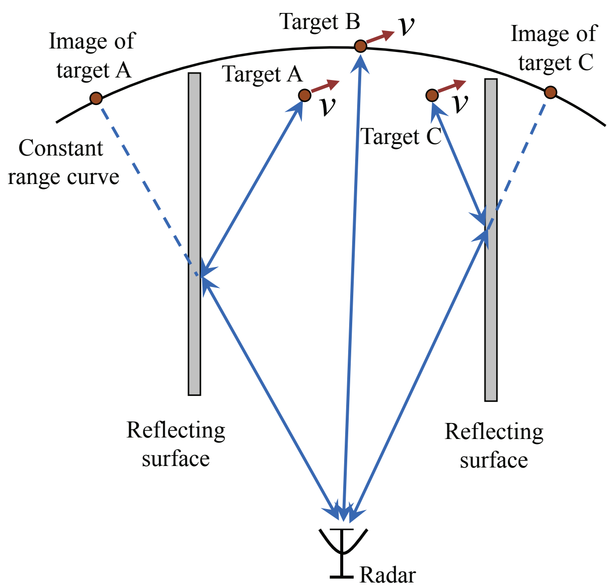

Fig. 1. A schematic representation of the multipath scenario.

DS and requires much less computation time. Finally, in Section V, we summarize our contributions and discuss some possible future work.

II. Problem Description and Modeling

Fig. 1 presents a schematic representation of the problem scenario. We consider a far-field point target in a multipath-rich environment, moving with a constant relative velocity $\boldsymbol{v}$ with respect to the radar. At the operating frequency we assume that the reflecting surfaces produce only specular reflections of the radar signal, and for simplicity we consider only the first-order reflections. We further assume that the radar has the complete knowledge of the environment that is under surveillance. This assumption implies that for a particular range cell (shown as the curved line in Fig. 1) the radar knows all the possible paths, be they LOS or reflected. Now, any target (e.g., Target B) or any image of a target (e.g., Target A or C) residing on the constant-range curved line has the same roundtrip delay and produces returns in the same range cell. Our goal here is to decide whether a target is present at the range cell under test.

We consider an OFDM signalling system with L active subcarriers, a bandwidth of B Hz, and pulse duration of T seconds. Let $\boldsymbol{a} = [a_0, a_1, \ldots, a_{L-1}]^T$ represent the complex weights transmitted over the L subcarriers, and satisfying $\sum_{l=0}^{L-1} |a_l|^2 = 1$. We incorporate information of the known range cell (denoted by the roundtrip delay τ) by substituting $t = \tau + nT_{\mathrm{P}}, n = 0, \ldots, N-1$, where T_{P} is the pulse repetition interval (PRI) and N is the number of temporal measurements within a given coherent processing interval (CPI). Then, corresponding to a specific range cell containing the target, the complex envelope of the received signal at the output of the l-th subchannel is

$$y_l(n) = a_l\, x_{lp}\, \phi_l(n, p, \boldsymbol{v}) + e_l(n), \tag{1}$$

where

- x_{lp} is a complex quantity representing the scattering coefficient of the target along the l-th subchannel and p-th path;
- $\phi_l(n, p, \boldsymbol{v}) \triangleq e^{-j2\pi f_l \tau}\, e^{j2\pi f_l \beta_p n T_{\mathrm{P}}}$;
- $\beta_p = 2\langle \boldsymbol{v}, \boldsymbol{u}_p \rangle / c$ is the relative Doppler shift along the p-th path;
- $\boldsymbol{u}_p$ represents the direction-of-arrival unit-vector of the p-th path;
- c is the speed of propagation; and
- $e_l(t)$ represents the clutter and measurement noise along the l-th subchannel.

Next, we discretize the possible signal paths and target velocities into P and V grid points, respectively. Restricting our operation to a narrow region of interest (e.g., an urban canyon where the range is much greater than the width) and a few class of targets that have comparable velocities (e.g., cars/trucks within a city environment), we can restrict the values of P and V to smaller numbers. Then, considering all possible combinations of $(p_i, \boldsymbol{v}_j), i = 1, 2, \ldots, P, j = 1, 2, \ldots, V$, we can rewrite (1) as

$$y_l(n) = a_l\, \boldsymbol{\phi}_l(n)^T \boldsymbol{x}_l + e_l(n), \tag{2}$$

where

- $\boldsymbol{\phi}_l(n) = [\phi_l(n, p_1, \boldsymbol{v}_1), \ldots, \phi_l(n, p_P, \boldsymbol{v}_V)]^T$; and
- $\boldsymbol{x}_l$ is a $PV \times 1$ sparse-vector, having only k_l nonzero entries corresponding to the true signal paths and target velocity.

Concatenating the measurements of all subchannels and temporal points we get

$$\boldsymbol{y} = \boldsymbol{\Phi}\, \boldsymbol{x} + \boldsymbol{e}, \tag{3}$$

where

- $\boldsymbol{y} = \left[\boldsymbol{y}(0)^T, \ldots, \boldsymbol{y}(N-1)^T\right]^T$ is an $LN \times 1$ vector with $\boldsymbol{y}(n) = [y_0(n), \ldots, y_{L-1}(n)]^T$;
- $\boldsymbol{\Phi} = \left[(\boldsymbol{A\Phi}(0))^T \cdots (\boldsymbol{A\Phi}(N-1))^T\right]^T$ is an $LN \times LPV$ matrix, containing all possible combinations of signal path and target velocity, with $\boldsymbol{A} = \mathrm{diag}(\boldsymbol{a})$ and $\boldsymbol{\Phi}(n) = \mathrm{blkdiag}\left(\boldsymbol{\phi}_0(n)^T, \ldots, \boldsymbol{\phi}_{L-1}(n)^T\right)$;
- $\boldsymbol{x} = \left[\boldsymbol{x}_0^T, \ldots, \boldsymbol{x}_{L-1}^T\right]^T$ is an $LPV \times 1$ sparse-vector that has $k = \sum_{l=0}^{L-1} k_l$ nonzero entries; and
- $\boldsymbol{e} = \left[\boldsymbol{e}(0)^T, \ldots, \boldsymbol{e}(N-1)^T\right]^T$ is an $LN \times 1$ vector, comprising of clutter returns, noise, and interference, with $\boldsymbol{e}(n) = [e_0(n), \ldots, e_{L-1}(n)]^T$.

In our problem, the clutter could be the contribution of undesired reflections from the environment surrounding or behind the target, or random multipath reflections from the irregularities on the reflecting surface (e.g., windows and balconies of the buildings in an urban scenario), that cannot be modeled as specular components. Therefore, following the central limit theorem, we assume that $\boldsymbol{e}(n)$ is a temporally white and circularly symmetric complex Gaussian vector, distributed as $\boldsymbol{e} \sim \mathbb{CN}_{LN}\left(\boldsymbol{0}, \boldsymbol{I}_N \otimes \boldsymbol{\Sigma}\right)$.

III. Sparse Recovery and Performance Analysis

In this section, we first develop a sparse recovery algorithm for the measurement model presented in the previous section. Then, we analytically evaluate its performance characteristics in terms of an upper bound on the ℓ_2-norm of the sparse-estimation error.

A. Sparse Recovery

The goal of a reconstruction algorithm is to estimate the vector $\boldsymbol{x}$ from the noisy measurement $\boldsymbol{y}$ by exploiting the sparsity. One of the most popular approaches of sparse signal recovery is the Dantzig selector (DS) that provides an estimate of $\boldsymbol{x}$ as a solution to the following ℓ_1-regularization problem:

$$\min_{\boldsymbol{z}\in\mathbb{C}^{LPV}} \|\boldsymbol{z}\|_1 \quad \text{subject to} \quad \left\|\boldsymbol{\Phi}^H(\boldsymbol{y}-\boldsymbol{\Phi}\boldsymbol{z})\right\|_\infty \le \lambda\cdot\sigma, \quad (4)$$

where $\lambda = \sqrt{2\,\log(LPV)}$ is a control parameter and $\sigma = \sqrt{\mathrm{tr}\Sigma/L}$.

However, from the discussion of the previous section we observe an additional structure in $\boldsymbol{x}$, described as follows:

$$\boldsymbol{x} = \left[\boldsymbol{x}_0^T, \boldsymbol{x}_1^T, \ldots, \boldsymbol{x}_{L-1}^T\right]^T, \quad (5)$$

where each $\boldsymbol{x}_l$, $l = 0,1,\ldots,L-1$, is sparse with sparsity level $k_l = \|\boldsymbol{x}_l\|_0$, and $k = \sum_{l=0}^{L-1} k_l$. Furthermore, the system matrix $\boldsymbol{\Phi}$ in (3) can also be expressed as

$$\boldsymbol{\Phi} = [\,\boldsymbol{\Phi}_0 \;\; \boldsymbol{\Phi}_1 \;\; \cdots \;\; \boldsymbol{\Phi}_{L-1}\,], \quad (6)$$

where each block-matrix, of dimension $LN \times PV$, is orthogonal to any other block-matrix; i.e., $\boldsymbol{\Phi}_{l_1}^H\boldsymbol{\Phi}_{l_2} = \boldsymbol{0}$ for $l_1 \ne l_2$. Note the difference in notation between $\boldsymbol{\Phi}_l$ (which is a columnwise block-matrix) and $\boldsymbol{\Phi}(n)$ (which is a rowwise block-matrix).

To exploit this additional structure in the sparse-recovery algorithm, we propose a better reconstruction algorithm that solves L small Dantzig selectors:

$$\min_{\boldsymbol{z}_l\in\mathbb{C}^{PV}} \|\boldsymbol{z}_l\|_1 \quad \text{subject to} \quad \left\|\boldsymbol{\Phi}_l^H(\boldsymbol{y}-\boldsymbol{\Phi}_l\boldsymbol{z}_l)\right\|_\infty \le \lambda_l\cdot\sigma, \quad (7)$$

where $\lambda_l = \sqrt{2\,\log(PV)}$ and $l = 0,1,\ldots,L-1$. We show in the next subsection that (7) has advantages over (4) both in terms of computation and performance, because more prior structures of the sparse vector are exploited.

B. Performance Analysis

To assess the reconstruction performance of an ℓ_1-based algorithm, in [9] we proposed a new, easily computable measure, ℓ_1-constrained minimal singular value (ℓ_1-CMSV) of $\boldsymbol{\Phi}$. According to [9, Def. 4], we define the ℓ_1-CMSV of $\boldsymbol{\Phi}$ as

$$\rho_s(\boldsymbol{\Phi}) = \min_{\boldsymbol{x}\ne\boldsymbol{0},\, s_1(\boldsymbol{x})\le s} \frac{\|\boldsymbol{\Phi}\boldsymbol{x}\|_2}{\|\boldsymbol{x}\|_2}, \quad \text{for any} \quad s \in [1, LPV], \quad (8)$$

where $s_1(\boldsymbol{x}) \triangleq \frac{\|\boldsymbol{x}\|_1^2}{\|\boldsymbol{x}\|_2^2} \le k$, when $k = \|\boldsymbol{x}\|_0$. Then, the performance of our decomposed DS in (7) is given by the following theorem:

Theorem 1. *Suppose $\boldsymbol{x} \in \mathbb{C}^{LPV}$ is a k-sparse vector having an additional structure as presented in (5), with each $\boldsymbol{x}_l \in \mathbb{C}^{PV}$ being a k_l-sparse vector, and (3) is the measurement model. Choose $\lambda_l = \sqrt{2\,\log(PV)}$ in (7). Then, with high probability, $\widehat{\boldsymbol{x}}$ satisfies*

$$\|\widehat{\boldsymbol{x}}-\boldsymbol{x}\|_2 \le 4\sqrt{\sum_{l=0}^{L-1} \frac{\lambda_l^2\, k_l\, \sigma^2}{\rho_{4k_l}^4(\boldsymbol{\Phi}_l)}}, \quad (9)$$

where the concentrated solution $\widehat{\boldsymbol{x}} = \left[\widehat{\boldsymbol{x}}_0^T, \widehat{\boldsymbol{x}}_1^T, \ldots, \widehat{\boldsymbol{x}}_{L-1}^T\right]^T$ is obtained by using the individual solutions, $\widehat{\boldsymbol{x}}_l$, of (7). More specifically, if $\lambda_l = \sqrt{2\,(1+q)\,\log(PV)}$ for each $q \ge 0$ is used in (7), the bound holds with probability greater than $1 - L\left(\sqrt{\pi\,(1+q)\,\log(PV)}\cdot(PV)^q\right)^{-1}$.

Proof: Let us define the unobserved measurements $\boldsymbol{y}_l = \boldsymbol{\Phi}_l\,\boldsymbol{x}_l + \boldsymbol{e}$. Note that due to the orthogonality of $\boldsymbol{\Phi}_l$s,

$$\begin{aligned}\boldsymbol{\Phi}_l^H(\boldsymbol{y}-\boldsymbol{\Phi}_l\,\boldsymbol{z}_l) &= \boldsymbol{\Phi}_l^H\left(\sum_{l'=0}^{L-1}\boldsymbol{\Phi}_{l'}\,\boldsymbol{x}_{l'} + \boldsymbol{e} - \boldsymbol{\Phi}_l\,\boldsymbol{z}_l\right),\\ &= \boldsymbol{\Phi}_l^T\,(\boldsymbol{\Phi}_l\,\boldsymbol{x}_l + \boldsymbol{e} - \boldsymbol{\Phi}_l\,\boldsymbol{z}_l),\\ &= \boldsymbol{\Phi}_l^T\,(\boldsymbol{y}_l - \boldsymbol{\Phi}_l\,\boldsymbol{z}_l).\end{aligned} \quad (10)$$

As a consequence, the L small Dantzig selectors in (7) are equivalent with

$$\min_{\boldsymbol{z}_l\in\mathbb{C}^{PV}} \|\boldsymbol{z}_l\|_1 \quad \text{subject to} \quad \left\|\boldsymbol{\Phi}_l^H(\boldsymbol{y}_l-\boldsymbol{\Phi}_l\boldsymbol{z}_l)\right\|_\infty \le \lambda_l\cdot\sigma \quad (11)$$
$$\text{for} \quad l = 0,1,\ldots,L-1.$$

Then, denoting the individual solutions of (7) as $\widehat{\boldsymbol{x}}_l$ and assuming $\left\|\boldsymbol{\Phi}_l^H\boldsymbol{e}\right\|_\infty \le \lambda_l$, from [9, Th. 2] we have

$$\|\widehat{\boldsymbol{x}}_l-\boldsymbol{x}_l\|_2 \le 4\,\frac{\lambda_l\sqrt{k_l}\,\sigma}{\rho_{4k_l}^2(\boldsymbol{\Phi}_l)}. \quad (12)$$

Hence, defining the concatenated estimate as $\widehat{\boldsymbol{x}} = \left[\widehat{\boldsymbol{x}}_0^T, \widehat{\boldsymbol{x}}_1^T, \ldots, \widehat{\boldsymbol{x}}_{L-1}^T\right]^T$, we get

$$\|\widehat{\boldsymbol{x}}-\boldsymbol{x}\|_2 = \sqrt{\sum_{l=0}^{L-1}\|\widehat{\boldsymbol{x}}_l-\boldsymbol{x}_l\|_2^2} \le 4\sqrt{\sum_{l=0}^{L-1}\frac{\lambda_l^2\,k_l\,\sigma^2}{\rho_{4k_l}^4(\boldsymbol{\Phi}_l)}}. \quad (13)$$

■

On the contrary, if we use the original DS in (4) to obtain an estimate $\widehat{\boldsymbol{x}}_{\text{DS}}$, then using [9, Th. 2] we get

$$\|\widehat{\boldsymbol{x}}_{\text{DS}}-\boldsymbol{x}\|_2 \le 4\,\frac{\lambda\sqrt{k}\,\sigma}{\rho_{4k}^2(\boldsymbol{\Phi})}, \quad (14)$$

where $k = \sum_{l=0}^{L-1} k_l$ and $\left\|\boldsymbol{\Phi}^H\boldsymbol{e}\right\|_\infty \le \lambda = \sqrt{2\,\log(LPV)}$. We now have the following theorem:

Theorem 2. *The L small Dantzig selectors in (7) perform better than the original Dantzig selector in (4) in the sense of* *a smaller upper bound on the ℓ_2-norm of the sparse-estimation error:*

$$4\sqrt{\sum_{l=0}^{L-1}\frac{\lambda_l^2\,k_l\,\sigma^2}{\rho_{4k_l}^4(\boldsymbol{\Phi}_l)}} \le 4\,\frac{\lambda\sqrt{k}\,\sigma}{\rho_{4k}^2(\boldsymbol{\Phi})}. \tag{15}$$

Proof: Consider vectors $\boldsymbol{z}_l \in \mathbb{C}^{PV}$ satisfying

$$s_1(\boldsymbol{z}_l) = \frac{\|\boldsymbol{z}_l\|_1^2}{\|\boldsymbol{z}_l\|_2^2} \le 4k_l, \tag{16}$$

and a long vector $\boldsymbol{z} \in \mathbb{C}^{LPV}$ obtained after concatenating these $\boldsymbol{z}_l$s. Then, using the Cauchy-Schwartz inequality, we get

$$\begin{aligned}
\|\boldsymbol{z}\|_1 &= \sum_{l=0}^{L-1}\|\boldsymbol{z}_l\|_1\,,\\
&\le 2\sum_{l=0}^{L-1}\sqrt{k_l}\,\|\boldsymbol{z}_l\|_2\,,\\
&\le 2\sqrt{\sum_{l=0}^{L-1}k_l}\sqrt{\sum_{l=0}^{L-1}\|\boldsymbol{z}_l\|_2^2}\,,\\
&= 2\sqrt{k}\,\|\boldsymbol{z}\|_2\,,
\end{aligned}$$

that is,

$$s_1(\boldsymbol{z}) = \frac{\|\boldsymbol{z}\|_1^2}{\|\boldsymbol{z}\|_2^2} \le 4k. \tag{17}$$

As a consequence, for any such constructed z, we have

$$\rho_{4k}^2(\boldsymbol{\Phi}) \le \frac{\boldsymbol{z}^H\,\boldsymbol{\Phi}^H\,\boldsymbol{\Phi}\,\boldsymbol{z}}{\boldsymbol{z}^H\,\boldsymbol{z}} = \sum_{l=0}^{L-1}\frac{\boldsymbol{z}_l^H\,\boldsymbol{\Phi}_l^H\,\boldsymbol{\Phi}_l\,\boldsymbol{z}_l}{\boldsymbol{z}^H\,\boldsymbol{z}}.$$

Taking a z_l such that $\|\boldsymbol{z}_l\|_2^2 = \omega_l \ge 0$ with $\|\boldsymbol{z}\|_2^2 = \sum_{l=0}^{L-1}\omega_l = 1$, and

$$\omega_l\,\rho_{4k_l}^2(\boldsymbol{\Phi}_l) = \boldsymbol{z}_l^H\,\boldsymbol{\Phi}_l^H\,\boldsymbol{\Phi}_l\,\boldsymbol{z}_l,$$

we get

$$\rho_{4k}^2(\boldsymbol{\Phi}) \le \sum_{l=0}^{L-1}\omega_l\,\rho_{4k_l}^2(\boldsymbol{\Phi}_l). \tag{18}$$

In particular, we have

$$\rho_{4k}^2(\boldsymbol{\Phi}) \le \rho_{4k_l}^2(\boldsymbol{\Phi}_l). \tag{19}$$

Moreover, noticing that $\lambda_l \le \lambda$, we obtain

$$\sum_{l=0}^{L-1}\frac{\lambda_l^2\,k_l\,\sigma^2}{\rho_{4k_l}^4(\boldsymbol{\Phi}_l)} \le \sum_{l=0}^{L-1}\frac{\lambda^2\,k_l\,\sigma^2}{\rho_{4k}^4(\boldsymbol{\Phi})} = \frac{\lambda^2\,k\,\sigma^2}{\rho_{4k}^4(\boldsymbol{\Phi})}. \tag{20}$$

■

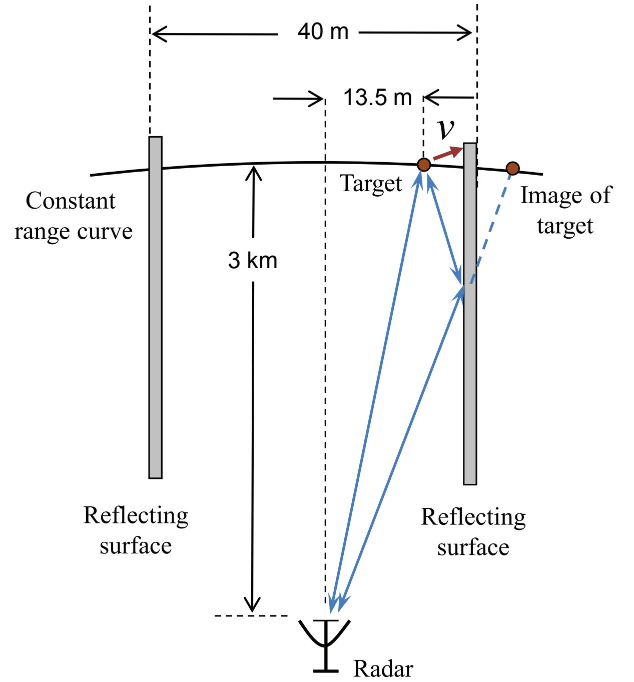

Fig. 2. A schematic representation of the multipath scenario considered in the numerical examples.

IV. Numerical Results

We present the results of several numerical examples to illustrate the sparse-estimation performance for a target-detection problem. Fig. 2 schematically describes a scenario that we used in the simulations. We simulated the situation of a range cell that is at a distance of 3 km from the radar (positioned at the origin). The target was 13.5 m east from the center line, moving with velocity $\boldsymbol{v} = (35/\sqrt{2})\,(\hat{i}+\hat{j})$ m/s. There were two different paths between the target and radar: one direct and one reflected, subtending angles of $0.26°$ and $0.51°$, respectively, with respect to the radar. We considered a 3-carrier OFDM radar operating with the following specifications: carrier frequency $f_c = 1$ GHz; bandwidth $B = 100$ MHz; pulse repetition interval $T_{\mathrm{P}} = 4$ ms; number of coherent pulses $N = 20$; and all the transmit OFDM weights were equal, i.e., $a_l = 1/\sqrt{L}\ \forall\, l$.

The scattering coefficients of the target, $\boldsymbol{x}$, were varied to simulate two different scenarios in our simulations. In Scenario 1, the target had equal scattering responses across all the subcarriers; i.e., $x_{l,\mathrm{d}}^{(1)} = [1,1,1]^T$ and $x_{l,\mathrm{r}}^{(1)} = [0.5,0.5,0.5]^T$ were the target scattering coefficients in Scenario 1 along the direct and reflected paths, respectively. In Scenario 2, we considered varying target-responses over different subcarriers; i.e., $x_{l,\mathrm{d}}^{(2)} = [4,1,2]^T$ and $x_{l,\mathrm{r}}^{(2)} = [2,0.5,2]^T$. We generated the noise samples from a $\mathbb{CN}(0,1)$ distribution, and then scaled the samples to satisfy the required target to clutter-plus-noise ratio (TCNR), defined as

$$\mathrm{TCNR} = \frac{\boldsymbol{x}^H\,\boldsymbol{x}}{N\,L\,\sigma_0^2}. \tag{21}$$

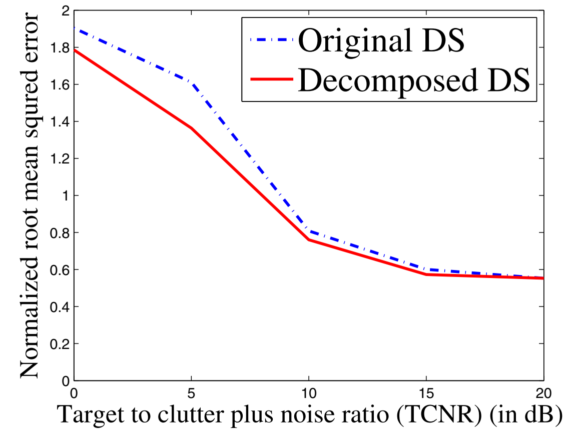

(a)

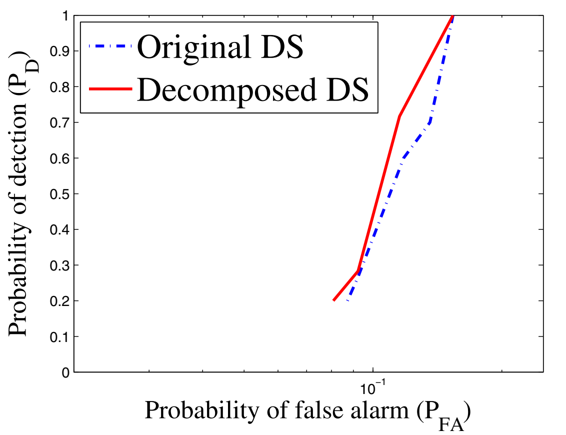

(b)

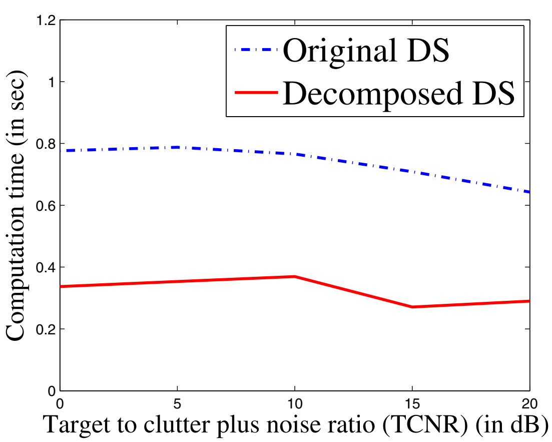

(c)

Fig. 3. Comparison of performances of the standard Dantzig selector and decomposed Dantzig selector in Scenario 1 in terms of (a) normalized RMSE, (b) empirical ROC, and (c) computation time with respect to target to clutter-plus-noise ratio.

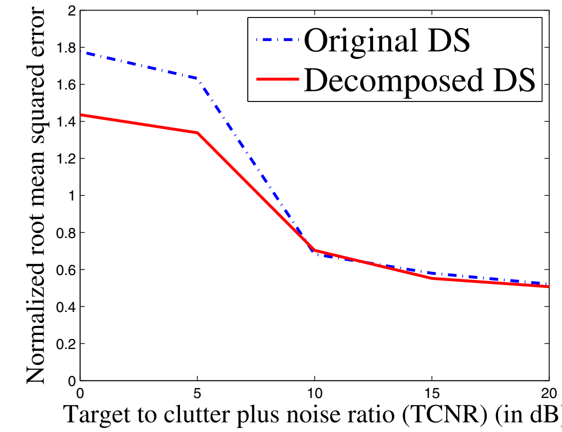

(a)

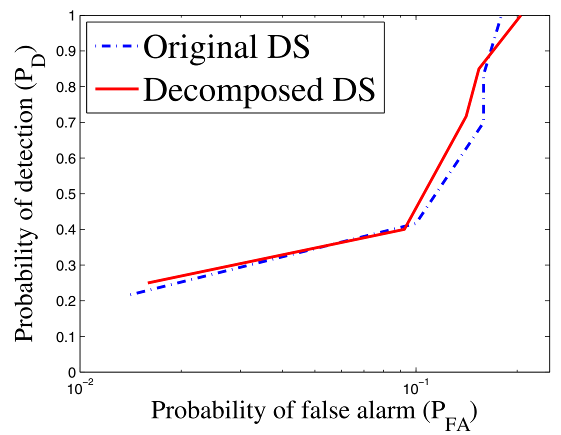

(b)

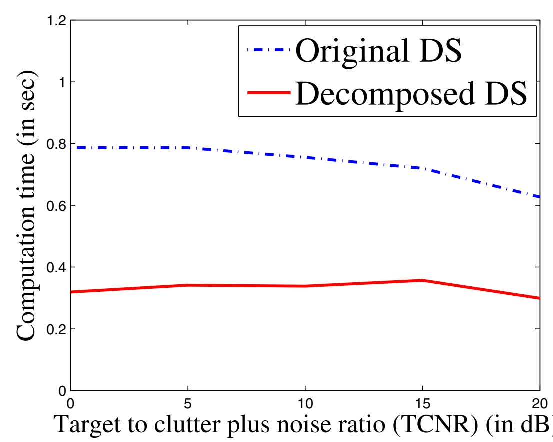

(c)

Fig. 4. Comparison of performances of the standard Dantzig selector and decomposed Dantzig selector in Scenario 2 in terms of (a) normalized RMSE, (b) empirical ROC, and (c) computation time with respect to target to clutter-plus-noise ratio.

Here we kept the clutter-plus-noise power the same across all the subcarriers by considering $\boldsymbol{\Sigma} = \sigma_0^2 \boldsymbol{I}_L$.

We partitioned the signal paths and target velocities into $P = 5$ and $V = 3$ uniform grid points. We considered signal paths that subtended angles of $\{-0.5°, -0.25°, 0°, 0.25°, 0.5°\}$ with respect to the radar and target velocities of $\{25, 35, 45\}$ m/s. Hence, according to our description in Section III, we had $k_l = 2\ \forall\, l$ and $k = 6$.

We analyzed the performance characteristics of our proposed technique in terms of the following two measures: (i) root mean squared error (RMSE), defined as $\|\widehat{\boldsymbol{x}} - \boldsymbol{x}\|_2$; and (ii) empirical receiver operating characteristic (ROC), computed using

$$P_{\mathrm{FA}} = \frac{n_{\mathrm{FA}}}{LPV - k}, \quad P_{\mathrm{D}} = \frac{n_{\mathrm{D}}}{k}, \tag{22}$$

where n_{T}, n_{D}, and $n_{\mathrm{FA}} = (n_{\mathrm{T}} - n_{\mathrm{D}})$ are the number of grid points corresponding to the estimated target response, detected grids within the set of true grid points, and the remaining grid points, respectively.

Figs. 3 and 4 show the performance characteristics in Scenario 1 and Scenario 2, respectively, at different TCNR values. We employed both the standard DS of (4) and our proposed decomposed DS of (7) to reconstruct the sparse vector. We notice that the decomposed DS performs better than the standard DS both in terms of normalized RMSE and empirical ROC, although the improvement is not huge apart from the low TCNR conditions. However, we get a drastic reduction in computation time (less than half of that required by the standard DS) using the decomposed DS.

V. Conclusions

In this paper, we proposed a sparsity-based estimation technique for detecting a moving target in the presence of multipath reflections. We first developed a parametric orthogonal frequency division multiplexing (OFDM) radar model for a particular range cell under test, and then converted it to a sparse model that accounts for the target returns over all possible signal paths and target velocities. The use of an OFDM signal increased the frequency diversity of our system, as different scattering centers of a target resonate variably at different frequencies. In our model, the nonzero components of the sparse vector correspond to the scattering coefficients of the target at different OFDM subcarriers. To estimate the sparse vector, we employed a collection of multiple small Dantzig selectors (DS) that exploit more prior structures of the sparse vector. We also analytically evaluated the performance characteristics of our decomposed DS algorithm using the ℓ_1-constrained minimal singular value (ℓ_1-CMSV) of the measurement matrix and showed that it performs better than the standard DS algorithm. We presented numerical examples to illustrate the performance characteristics of the sparse recovery. In our future work, we will extend our model to incorporate more realistic physical effects, such as diffractions and refractions. We will incorporate different waveform design criteria to further improve the detection performance.

References

[1] S. Sen, M. Hurtado, and A. Nehorai, "Adaptive OFDM radar for detecting a moving target in urban scenarios," in *Proc. 4th Int. Waveform Diversity & Design (WDD) Conf.*, Orlando, FL, Feb. 8–13, 2009, pp. 268–272.

[2] S. Sen and A. Nehorai, "Adaptive OFDM radar for target detection in multipath scenarios," *IEEE Trans. Signal Process.*, vol. 59, no. 1, pp. 78–90, Jan. 2011.

[3] T. May and H. Rohling, "Orthogonal frequency division multiplexing," in *Wideband Wireless Digital Communications*, A. F. Molisch, Ed., chapter 17-25. Prentice Hall PTR, Upper Saddle River, NJ, 2001.

[4] S. Sen, G. Tang, and A. Nehorai, "Multi-objective optimization of OFDM radar waveform for target detection," *IEEE Trans. Signal Process.*, vol. 59, no. 2, pp. 639–652, Feb. 2011.

[5] S. S. Chen, D. L. Donoho, and M. A. Saunders, "Atomic decomposition by basis pursuit," *SIAM Jour. on Scientific Computing*, vol. 20, no. 1, pp. 33–61, Aug. 1998.

[6] D. Malioutov, M. Çetin, and A. S. Willsky, "A sparse signal reconstruction perspective for source localization with sensor arrays," *IEEE Trans. Signal Process.*, vol. 53, no. 8, pp. 3010–3022, Aug. 2005.

[7] E. Candès and T. Tao, "The Dantzig selector: Statistical estimation when p is much larger than n," *The Annals of Statistics*, vol. 35, no. 6, pp. 2313–2351, 2007.

[8] R. Tibshirani, "Regression shrinkage and selection via the lasso," *Journal of the Royal Statistical Society. Series B (Methodological)*, vol. 58, no. 1, pp. 267–288, 1996.

[9] G. Tang and A. Nehorai, "Performance analysis of sparse recovery based on constrained minimal singular values," submitted for publication, *ArXiv e-prints* available.

[10] E. J. Candès and T. Tao, "Decoding by linear programming," *IEEE Trans. Inf. Theory*, vol. 51, no. 12, pp. 4203–4215, Dec. 2005.

[11] E. J. Candès, "The restricted isometry property and its implications for compressed sensing," *Comptes Rendus Mathematique*, vol. 346, no. 9-10, pp. 589–592, May 2008.